



**HAL**  
open science

## Reconstructing Green's function by correlation of the coda of the correlation (C3) of ambient seismic noise

L. Stehly, Michel Campillo, B. Froment, R. L. Weaver

### ► To cite this version:

L. Stehly, Michel Campillo, B. Froment, R. L. Weaver. Reconstructing Green's function by correlation of the coda of the correlation (C3) of ambient seismic noise. *Journal of Geophysical Research : Solid Earth*, 2008, 113 (B11306), 1 à 10 p. 10.1029/2008JB005693 . insu-00372156

**HAL Id: insu-00372156**

**<https://insu.hal.science/insu-00372156>**

Submitted on 5 Mar 2021

**HAL** is a multi-disciplinary open access archive for the deposit and dissemination of scientific research documents, whether they are published or not. The documents may come from teaching and research institutions in France or abroad, or from public or private research centers.

L'archive ouverte pluridisciplinaire **HAL**, est destinée au dépôt et à la diffusion de documents scientifiques de niveau recherche, publiés ou non, émanant des établissements d'enseignement et de recherche français ou étrangers, des laboratoires publics ou privés.

## Reconstructing Green's function by correlation of the coda of the correlation ( $C^3$ ) of ambient seismic noise

L. Stehly,<sup>1,2,3</sup> M. Campillo,<sup>1</sup> B. Froment,<sup>1</sup> and R. L. Weaver<sup>4</sup>

Received 16 March 2008; revised 20 June 2008; accepted 22 July 2008; published 21 November 2008.

[1] Analysis of long-range correlation of the microseisms has been shown to provide reliable measurements of surface wave speeds that can be used for seismic imaging and monitoring. In the case of an even distribution of noise sources, it has been theoretically demonstrated that the correlation is the exact Green's function, including all types of waves. This method is limited in its application by the actual source distribution. In practice, the azimuthal distribution of energy flux of the noise is dominated by some particular directions resulting in a clear azimuthal dependence of the quality of the reconstruction of Rayleigh waves, with a poor reconstruction in some azimuths. To solve this problem, we use noise correlations measured on the entire network. We consider two stations, A and B, for which the Rayleigh waves could not be discerned in the correlation of continuous records of ambient noise. We computed all correlations between the station A (respectively B) and all the 150 other stations located at regional distances. Theoretically, these virtual seismograms contain direct waves and coda, although they are clearly contaminated by the influence of the imperfect ambient noise field and most are inadequate for direct analysis. We used these correlation functions as equivalents to seismograms produced by sources acting at the 150 stations locations and recorded in A (respectively B). We select time windows in those virtual seismograms that correspond to coda and compute correlations between them. This metacorrelation is found to exhibit the surface wave part of the Green's function that was not visible in the raw correlation of ambient noise. We illustrate the legitimacy of the reconstruction by comparison with raw noise correlations. This procedure can be used to assess seismic velocity between stations, even in presence of a directive and poorly oriented ambient noise. The result shows that in spite of the small signal-to-noise ratios often seen in correlations of ambient noise, especially at large lag time corresponding to coda, their codas are better equipartitioned than was the ambient noise upon which they were based. They are therefore presumably multiply scattered and contain information on both direct surface waves and also on more complex travel paths.

**Citation:** Stehly, L., M. Campillo, B. Froment, and R. L. Weaver (2008), Reconstructing Green's function by correlation of the coda of the correlation ( $C^3$ ) of ambient seismic noise, *J. Geophys. Res.*, 113, B11306, doi:10.1029/2008JB005693.

### 1. Introduction

#### 1.1. Reconstruction of the Green's Function From Correlations of Random Fields

[2] The correlation of long time series of seismic ambient noise makes possible the empirical synthesis of the earth response (Green's function) between the stations. It was shown to be an efficient tool for seismic tomography [Shapiro *et al.*, 2005; Sabra *et al.*, 2005b; Yao *et al.*, 2006; Yang *et al.*, 2007; Lin *et al.*, 2007; Brenguier *et al.*, 2007].

These studies were based upon the analysis of direct surface waves. In practice, it is difficult to assess unambiguously the presence of other types of waves (body waves, reflected or scattered waves, etc.). Nevertheless, from a theoretical point of view, the Earth response (Green's function) between two points can be retrieved from observations of apparently random fields, in absence of a deterministic source at one of the points. This is similar to the fluctuation-dissipation theorem, and Weaver and Lobkis [2001] have demonstrated experimentally that the cross correlation of the thermal noise recorded at two piezoelectric sensors at the surface of an aluminum sample leads to the complete Green's function between these two points. The same principles were successfully applied for local helioseismology [e.g., Duvall *et al.*, 1993; Gizon and Birch, 2004, 2005]. For microseism records, the randomness could be produced both by the distribution of sources and by scattering of seismic waves by topography and internal heterogeneities.

<sup>1</sup>LGIT, Université Joseph Fourier and CNRS, Grenoble, France.

<sup>2</sup>CEA/DASE, Bruyères-le-Châtel, France.

<sup>3</sup>Now at Berkeley Seismological Laboratory, University of California, Berkeley, California, USA.

<sup>4</sup>Department of Physics, University of Illinois at Urbana-Champaign, Urbana, Illinois, USA.

[3] An extreme case of randomness is provided in an arbitrary medium by an homogeneous distribution of white noise sources. *Weaver and Lobkis* [2004], Y. Colin de Verdière (Mathematical models for passive imaging. I: General background, 2006, available at <http://fr.arxiv.org/abs/math-ph/0610043/>), *Weaver* [2008], and *Snieder* [2007] demonstrated that in this case the correlation  $C$  between the displacement fields  $u(t, \mathbf{r})$  in  $A$  and  $B$  verifies

$$\frac{d}{d\tau} C(\tau, \mathbf{r}_A, \mathbf{r}_B) = \frac{-\sigma^2}{4a} (G(\tau, \mathbf{r}_A, \mathbf{r}_B) - G(-\tau, \mathbf{r}_A, \mathbf{r}_B)) \quad (1)$$

In expression (1),  $\tau$  is the correlation lag time,  $G$  is the Green's function of the absorbing medium,  $a(\mathbf{r})$  is a coefficient of attenuation, and  $\sigma$  is the variance of the source distribution. Note that  $G$  represents the exact Green's function of the medium, including all types of waves. This is a generalization of the results of *Lobkis and Weaver* [2001] for a finite body and *Roux et al.* [2005] for an homogeneous body. Expression (1) is general in terms of complexity of the medium but limited in its practical application by the assumption of an homogeneous distribution of white noise sources. Other derivations [*Wapenaar*, 2004; *Snieder*, 2004; *Sánchez-Sesma et al.*, 2006] of expressions like (1) make comparable assumptions about the field being correlated or about its source.

[4] In practice, the scattering of seismic waves in the Earth plays an important role in the Green's function reconstruction by compensating for the lack of sources. The correlation of a diffuse wavefield converges to the complete Green's function of the medium [e.g., *Lobkis and Weaver*, 2001] through a relation essentially similar to equation (1).

[5] In practice, the scattering of seismic waves in the Earth plays an important role in the Green's function reconstruction by compensating for the lack of sources. Experimental evidence shows that multiple scattering in the Earth is sufficient to lead to regional equipartition [*Shapiro et al.*, 2000; *Hennino et al.*, 2001; L. Margerin et al., Energy partition of seismic coda waves in layered media: Theory and application to pinyon flats observatory, submitted to *Geophysical Journal International*, 2008]. Once the field is equipartitioned (all eigenmodes of the medium are excited with the same level of energy and a random phase), the correlation of the wavefield between two points converges to the Green's function between these two points [*Lobkis and Weaver*, 2001; *Sánchez-Sesma et al.*, 2006]. In a finite body, equipartition amongst the body's modes follows naturally from simple assumptions and random reflections and scattering. In an open medium such as the earth these arguments do not apply, and one must appeal to concepts of local modes and equipartition amongst them as enforced by multiple random scattering. It is therefore natural that Green's function can also be extracted from the long-range correlation of coda waves [*Campillo and Paul*, 2003; *Paul et al.*, 2005; *Yao et al.*, 2006]. Reviews on the correlation of seismic noise and coda waves are given by *Campillo* [2006], *Larose et al.* [2006], and *Gouédard et al.* [2008].

## 1.2. Practical Limitations of Noise Correlations

[6] Even though ambient noise correlations have been successfully used in seismology in tomographic studies

[e.g., *Shapiro et al.*, 2005; *Sabra et al.*, 2005b] and to monitor velocity changes [*Brenguier et al.*, 2008; *Wegler and Sens-Schönfelder*, 2007; *Sens-Schönfelder and Wegler*, 2006], it has become clear that Green's function reconstruction is not perfect even when correlating several years of noise. Two main reasons explain this discrepancy.

[7] First, the distribution of noise sources is not homogeneous as assumed in equation (1). Thus the correlations converge to a function  $R$  that can be different from the actual Green's function of the medium  $G$ . At period larger than 1 s, the seismic noise is generated by the permanent agitation of the oceans. The exact mechanism of coupling between the ocean and the solid Earth is still in debate since the theoretical background was set by *Longuet-Higgins* [1950]. Observations indicate that the sources of seismic noise in the band 5–50 s are in the oceans and depend strongly on season [e.g., *Stehly et al.*, 2006; *Kedar et al.*, 2008]. Even when averaged over 1 year the seismic noise recorded anywhere on the continents originates from a limited range of azimuths; the energy flux of the noise is not isotropic. Seismic ambient noise is not due to an homogeneous distribution of white noise sources as assumed to establish equation (1). This causes errors in Green's function reconstruction. Even the fundamental modes of surface waves can be difficult to extract when the station pair is badly oriented with respect to the predominant direction of energy flux of the noise. For this reason tomographic studies usually use fewer than one third of the paths.

[8] Secondly, as finite length noise records are used, the convergence of the correlations toward the function  $R$  is not complete, and fluctuations remains in the correlations. The convergence toward the Green's function, i.e., the ratio of amplitude of  $R$  over residual fluctuations, is evolving as the square root of the amount of data used in the cross correlation [*Larose et al.*, 2004; *Snieder*, 2004; *Sabra et al.*, 2005a; *Weaver and Lobkis*, 2005]. This is guaranteed only when the field is due to uniformly distributed random sources, or when the field is due to equipartitioned incident waves. Using finite length records cause remaining fluctuations around the Greens function that are significant, in practice, making it difficult to identify other arrivals than the predominant fundamental mode of surface waves (body waves, higher mode, reflected waves, etc.).

[9] Identification of  $C$  and  $G$  thus depends on a sufficiently long record of ambient noise and assumptions on the nature of that noise. It is of particular noteworthiness here that some have correlated seismic coda with a degree of success [*Campillo and Paul*, 2003; *Paul et al.*, 2005]. Coda, being multiply scattered [*Hennino et al.*, 2001] does not suffer from the first of the above sources of discrepancy. It does, however suffer heavily from the first; coda records are short and rare. Ambient noise, in contrast, suffers from the first but not the second. The aim of this paper is to propose a technique to construct the Green's function from records that are both long and equipartitioned. It relies on both long term averaging of noise correlation and the properties associated with the diffuse character of the coda waves of the raw correlations. This new method allows us to reconstruct the Greens function for station pairs for which raw noise correlation is inadequate. The efficiency of this approach is an indirect demonstration that raw noise

correlation contains the scattered wave part of the Green's function.

## 2. $C^3$ : Correlation of Coda Waves Reconstructed by Noise Correlations

### 2.1. Method: Example of the Path EMV-GIMEL

[10] Our first aim is to see if it is possible to reconstruct the Green's function between distant stations pairs by correlating coda waves reconstructed by noise correlations, without contributions from reconstructed direct waves. For sake of simplicity, we call ' $C^3$  function' the Correlation of Coda of Correlation. To test this method we compare the Green's function obtained by correlating 1 year of noise and the  $C^3$  function.

[11] We use pairs of stations in the Alps which are part of a regional network of 150 broadband stations. We make a first estimate of the Green's function between each station pairs by correlating 1 year of vertical continuous records of seismic ambient noise. The noise correlations are performed in the following way: (1) First the records are decimated to 1 Hz and the instrument responses are deconvolved, (2) the spectrum of all the noise records are whitened between 5 and 150 s, and (3) for each station pair we correlate the noise records day per day, and stack all the daily correlations to obtain the final result.

[12] Figure 1c shows the Green's function in red reconstructed for the path EMV-GIMEL in the two period bands 5–10 s and 10–20 s. The interstation distance is 71 km. The positive time of the noise correlation corresponds to the causal Green's function of the medium between EMV and GIMEL, and the negative time corresponds to its anticausal counterpart (i.e., the Green's function between GIMEL and EMV). A wave train corresponding to Rayleigh waves is clearly visible on the two period bands in the positive and negative correlation time at 30 s. This corresponds to a velocity of 2.6 km/s.

[13] Now we show that it is possible to reconstruct the Green's function between EMV and GIMEL by another way. Let us call  $S$  a third station of the network used:

[14] 1. We compute the noise correlation between EMV (respectively GIMEL) and the station  $S$ . We identify the result as the Green's function between EMV (GIMEL) and the station  $S$ , that is the vertical records that we would get at EMV if we put a vertical source at  $S$  or vice versa. The station  $S$  plays the role of a "virtual source."

[15] 2. We select the time window that corresponds to the coda wave part of the Green's function of the noise correlation between EMV (respectively GIMEL) and  $S$ . This mean that we do not use at all the prominent direct arrival of the Rayleigh wave that is clearly visible on the noise correlation. We define the coda window as a 1200 s window beginning at two times the Rayleigh wave travel time. We decided to use a 1200 s windows after having tested several windows length, since it maximizes the signal-to-noise ratio of the result. We select the coda both in the positive and negative correlation time.

[16] 3. In a way similar to that of *Campillo and Paul* [2003], we cross correlate the coda selected on the EMV-S and GIMEL-S noise correlation. Note that we compute four different correlations, as we use the coda in both the positive and negative correlation time. We correlate the coda of the

positive time of the EMV-S and GIMEL-S noise correlation together  $C_{PP}^3$ , as well as the negative times ( $C_{NN}^3$ ), and also the positive times with the time reversed negative times ( $C_{PN}^3$ ), and the time reversed negative times with the positive times ( $C_{NP}^3$ ).

[17] 4. We average the four correlations over the 100 stations that compose the networks to get the four intermediate  $C_{II}^3$  functions.

[18] 5. We stack the four intermediates  $C_{II}^3$  functions to get the resulting  $C^3$  function.

### 2.2. Results for the Path EMV-GIMEL

[19] The result is presented in Figure 1 where we compare the Green's function between EMV and GIMEL reconstructed by correlating directly the noise recorded at these two stations and the  $C^3$  functions in the two period bands 5–10 s and 10–20 s. Figure 1b shows the noise correlation in black, and the four intermediate  $C_{II}^3$  functions averaged on all the 100 stations of the network with colored lines. Figure 1c shows the stack of the four intermediate  $C_{II}^3$  functions in red and the noise correlation in blue.

[20] The agreement between the  $C^3$  functions and the noise correlation for the direct Rayleigh wave is striking in the two period bands and for both positive and negative time. We measure exactly the same arrival time, and the waveforms are similar. This result shows that it is possible to reconstruct the Green's function between a pair of distant stations by computing the  $C^3$  functions (i.e., by correlating the coda waves reconstructed by noise correlation). This proves that individual noise correlation contains different parts of the Green's function, including multiply scattered waves. These waves are not usually visible on a single correlation due to the large remnant fluctuations. It is remarkable to notice that the cumulative duration of the coda waves used to compute the  $C^3$  function is 100 times smaller than the duration of the noise records used for the noise correlation. It was already noticed in previous studies that coda waves correlations converge more quickly to the Green's function than noise correlations.

[21] One can notice the different amplitudes of the intermediate  $C_{II}^3$  function. The highest amplitude are corresponding to  $C_{PP}^3$  and  $C_{NN}^3$ . The direct Rayleigh wave is even not visible in  $C_{NP}^3$  and  $C_{PN}^3$  in some cases (see Figure 1b, the negative times for the 10–20 s period band). We interpret these differences as the result of the time asymmetry of the initial noise correlation. As a matter of fact the noise in our region of study is dominated by the contribution of sources in the North Atlantic [e.g., *Stehly et al.*, 2006; *Kedar et al.*, 2008]. The noise correlation GIMEL-S or EMV-S are therefore expected to be asymmetric in most of the cases due to this preferential flux of energy. The reconstructed coda parts of the Green's functions are expected to exhibit the same amplitude asymmetry (see the discussion of the anisotropic flux of finite lapse time coda waves by *Paul et al.* [2005]). Therefore, if for example the largest amplitude of the noise correlation GIMEL-S or EMV-S is in positive time, and since correlation corresponds to a spectral multiplication, the coda correlation  $C_{PP}^3$  will have the largest amplitude among the intermediate  $C_{II}^3$ . Indeed, for noise correlations with another station  $S$ , the maximum amplitude can be for negative time and therefore the largest contribution is for  $C_{NN}^3$ . The strong asymmetry of the noise correlations results in a predominance

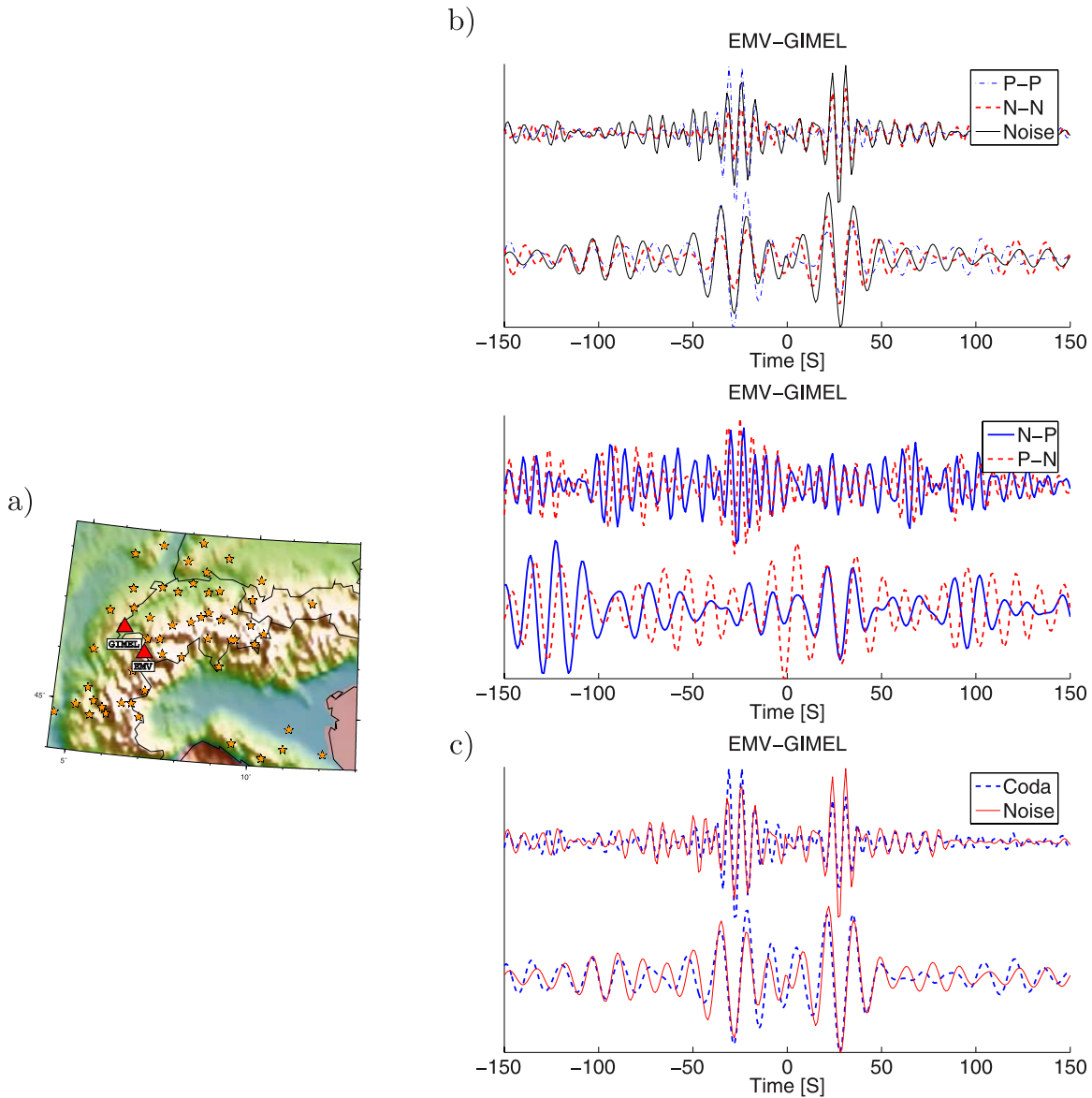


**Figure 1.** (a) Map of Switzerland and surrounding areas, with orange stars showing the stations  $S$  used to reconstruct the Green's function between EMV and GIMEL (red triangle). (b) (top) Green's function between EMV and GIMEL reconstructed by correlating 1 year of noise records (black) and by correlating coda waves reconstructed by noise correlations (colors). We show the two intermediates  $C_{II}^3$  functions where for each station  $S$  of the network, the coda of the noise correlation for the path EMV- $S$  and GIMEL- $S$  was selected on the positive noise correlation time (positive-positive,  $C_{PP}^3$ , blue dash-dotted line) and on the negative time (negative-negative,  $C_{NN}^3$ , red dashed line). Two period band are shown 5–10 s (first trace) and 10–20 s (second trace). (bottom) The two intermediates functions  $C_{NP}^3$  (blue solid line) and  $C_{PN}^3$  (red dashed line). (c) Noise correlation function between EMV and GIMEL (solid black line) and the stack of the four intermediate  $C_{II}^3$  functions shown with colored lines on Figure 1b (dashed blue line). Two period bands are shown 5–10 s (first trace) and 10–20 s (second trace).

of  $C_{PP}^3$  and  $C_{NN}^3$  over the other terms when averaged over the set of the  $S$  stations of the network. The  $C_{NP}^3$  and  $C_{PN}^3$  functions may have a very low signal-to-noise ratio and therefore their contributions to  $C^3$  do not improve the quality of the reconstruction of the Green's function. For this reason, in sections 2.3–4 we stacked only the  $C_{PP}^3$  and  $C_{NN}^3$  function to get the  $C^3$  function.

### 2.3. Range Time Representation of $C^3$ Functions

[22] The successful reconstruction of the Green's function by correlating coda waves reconstructed by noise correlation was not limited to the path EMV-GIMEL. We computed the  $C^3$  functions for 1200 paths whose range was between 50 and 300 km, in the three period bands 5–10 s, 10–20 s, and 20–40 s. We selected the best waveforms using a signal-to-noise ratio criteria. We define the signal-

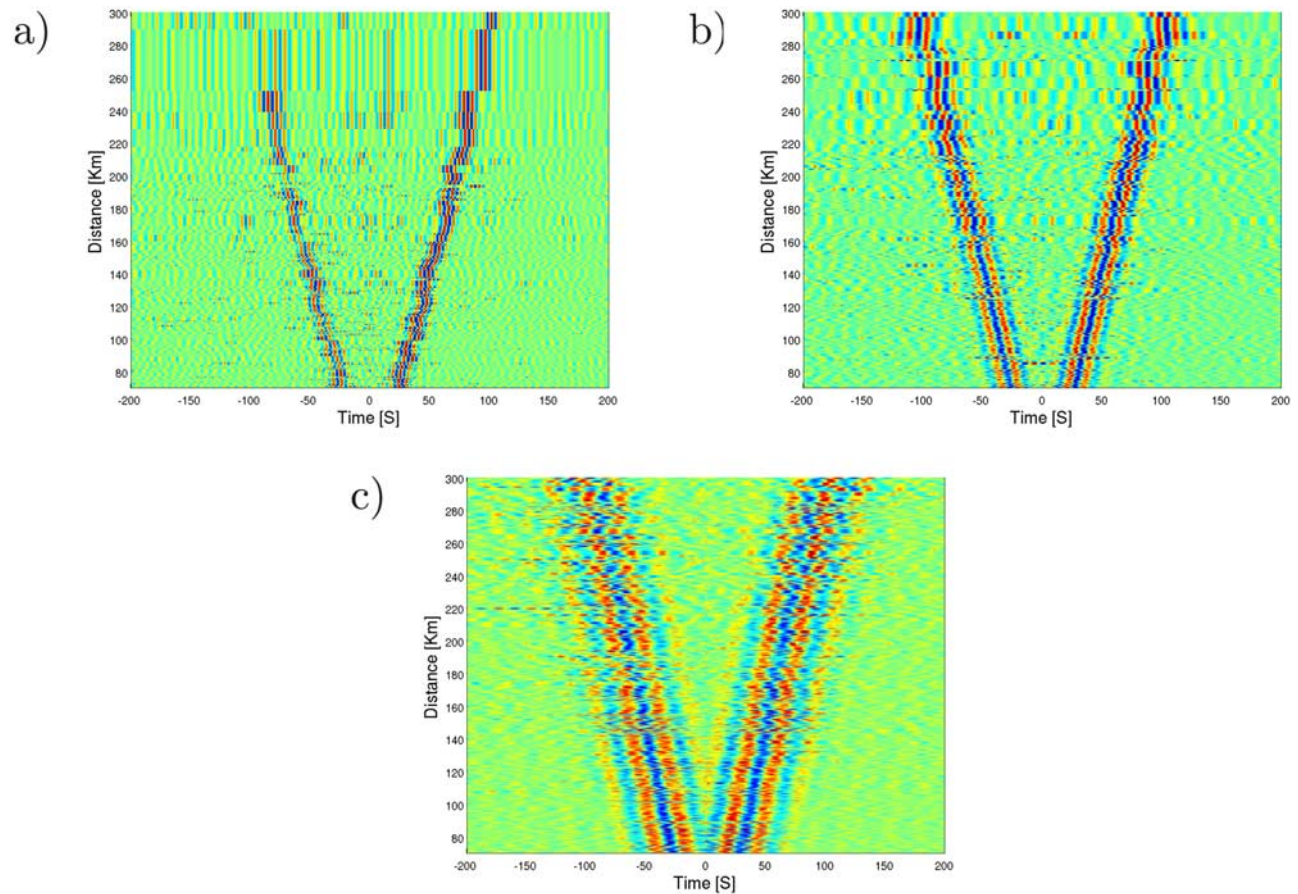


**Figure 2.** Range time representation of  $C^3$  functions in the period bands (a) 5–10 s, (b) 10–20 s, and (c) 20–40 s.

to-noise ratio of the  $C^3$  function as the ratio of the amplitude of the Rayleigh wave and the variance of the noise preceding the direct Rayleigh wave. More precisely, the variance of the noise is evaluated in a time window that starts at times 0 and finishes at the times corresponding to a velocity of  $5 \text{ km s}^{-1}$  (i.e., if the interstation distance is 300 km, the standard deviation of the noise is evaluated in a time window from 0 to 60 s). We kept waveforms whose signal-to-noise ratio was superior or equal to 7 in either the positive or negative correlation time. Figure 2 shows the range time representation of the best  $C^3$  functions for the three period bands 5–10 s, 10–20 s, and 20–40 s. The  $C^3$  functions were flipped so that the highest amplitude is always on the positive correlation time. In the 5–10 s period band 145 paths were selected, in the 10–20 s we kept 343 paths, and 280 paths in the 20–40 s period band.

#### 2.4. Interpretation

[23] Why does the correlation of coda waves reconstructed by noise correlations averaged over 100 stations lead to the direct wave part of the Green's function that is as clean as the one obtained from noise correlations? This result may seem surprising since coda waves are not clearly visible on noise correlations.

[24] Ideally, with homogeneously distributed noise sources and with infinitely long noise records, noise correlations yield the actual Green's function  $G$  of the medium. However, in practice, noise correlations of long time records are

composed of the sum of two signals: the actual Green's function of the medium  $G$  and fluctuations that are not a part of the physical signal. These fluctuations are mainly due to the uneven distribution of noise sources with non delta-like autocorrelations time functions. The correlation converges to a function  $R$  that is different from the actual Green's function of the medium  $G$ . Moreover, as we use finite length noise records, the convergence of the correlations toward the function  $R$  is not complete, causing additional fluctuations in the correlation.

[25] The fluctuations observed before the direct arrival can be interpreted as the result of incoming plane waves with azimuth different from the strike of the two stations. These contributions would disappear in presence of an isotropic distribution of plane waves. Fluctuations in the correlation for times larger than the travel time of the dominant surface wave are associated, in practice, with the properties of the sources of the noise. Fluctuations not pertaining to the actual Green's function could be due to the fact that sources at a given location are not  $\delta$ -correlated in time but have intrinsic correlations due for example to the propagating nature of oceanic waves. Another origin could be that the contributed sources are located in a limited distance range in the direction of the stations. It would result in spurious contributions to the correlations associated with the correlation between arrivals corresponding to different modes of propagation (such as body waves and surface waves).

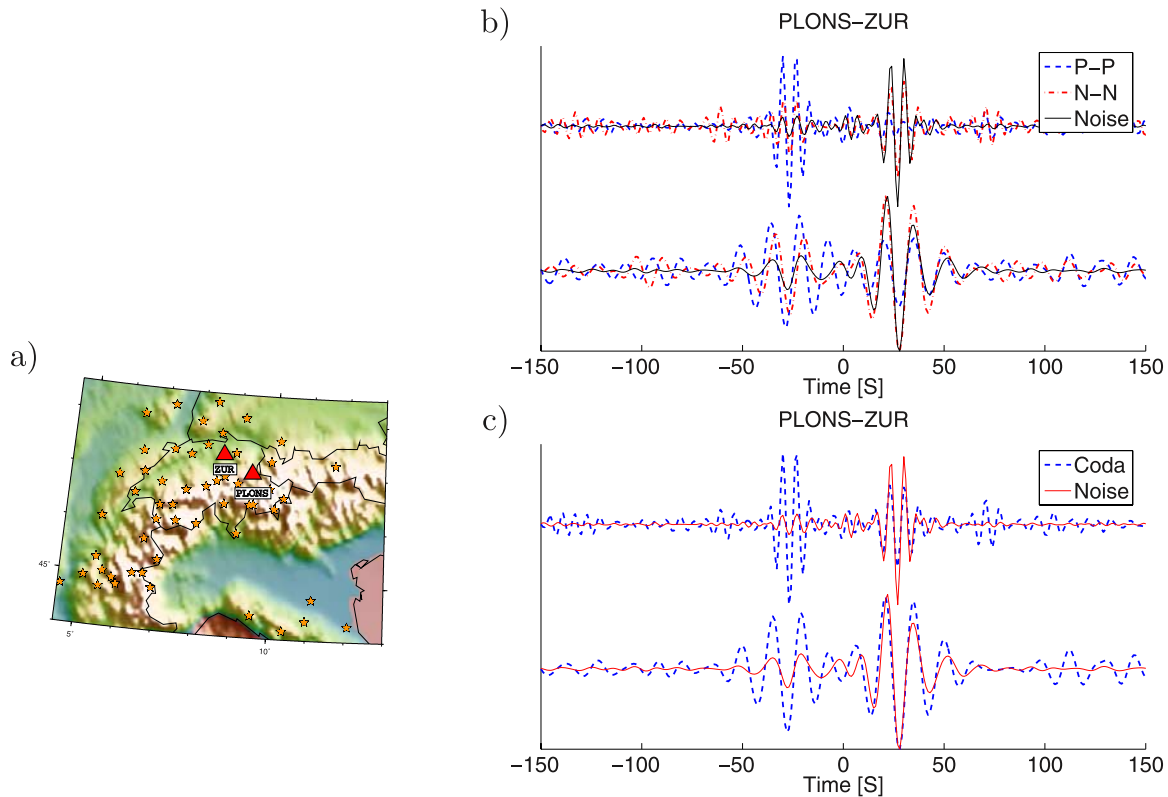


**Figure 3.** (a) Map of Switzerland and surrounding areas, with orange stars showing the stations  $S$  used to reconstruct the Green's function between PLONS and ZUR (red triangle). (b) Green's function between PLONS and ZUR reconstructed by correlating 1 year of noise records (solid black line) and by correlating coda waves reconstructed by noise correlations (colors). We show with different colors the 2 intermediate  $C_H^3$  functions where for each station  $S$  of the network, the coda of the noise correlation for the path PLONS- $S$  and ZUR- $S$  was selected on the positive noise correlation time (positive-positive, blue dashed line), on the negative time (negative-negative red dash-dotted line). (c) Noise correlation function between PLONS and ZUR (red) and the stack of the 2  $C_H^3$  functions (dashed blue) shown in colored line on the upper panel. Two period bands are shown at 5–10 s (first trace) and 10–20 s (second trace).

[26] For each of the initial correlations of noise (let us say between EMV or GIMEL and another station of the network in our case), these fluctuations are associated with the sources of noise in a specific region of origin in the strike of the two receivers. When stacking over the different paths, we average over different source regions, at different distances and with different time correlations. This average therefore tends to suppress the independent fluctuations and enhance the signals associated with the correlation of diffuse coda waves, that is the Green's function. As a consequence, it is possible to extract clear direct arrivals from late windows of the correlation in which coda are apparently dominated by random fluctuations.

[27] This experiment indirectly demonstrates that the long-range correlations contain more than direct surface waves and that even multiply scattered waves are present and can be themselves be used to construct ballistic arrivals.

### 3. Can We Gain Information by Recorrelating the Correlations?

#### 3.1. Example of the Path PLONS-ZUR

[28] Results presented in Figure 1 show that the correlations of correlations lead to a similar Green's function

reconstruction that noise correlations. One can ask if computing  $C^3$  functions could also be useful to retrieve the Green's function between station pairs that cannot be obtained from noise correlations.

[29] Figure 3 presents a comparison between the Green's function for the path PLONS-ZUR obtained from noise correlations and the one obtained from  $C^3$  functions, for the two period band 5–10 s and 10–20 s. The noise correlation is not symmetric: in the 5–10 s period band, the Green's function is only visible on positive correlation times and not in negative correlation times. In the 10–20 s period band, the amplitude and the signal-to-noise ratio is larger for positive correlation time (Figure 3b, black line). In practice, for tomographic studies only correlations that are symmetric in time with a good signal-to-noise ratio on both positive and negative sides are used. Otherwise it is not possible to guarantee that the Green's function was accurately reconstructed. For this reason the path PLONS-ZUR would not have been used.

[30] On the other hand the  $C^3$  function is symmetric: the Green's function is visible for both positive and negative correlation time with a similar signal-to-noise ratio for the two period bands 5–10 s and 10–20 s (Figure 3c, blue dashed line).

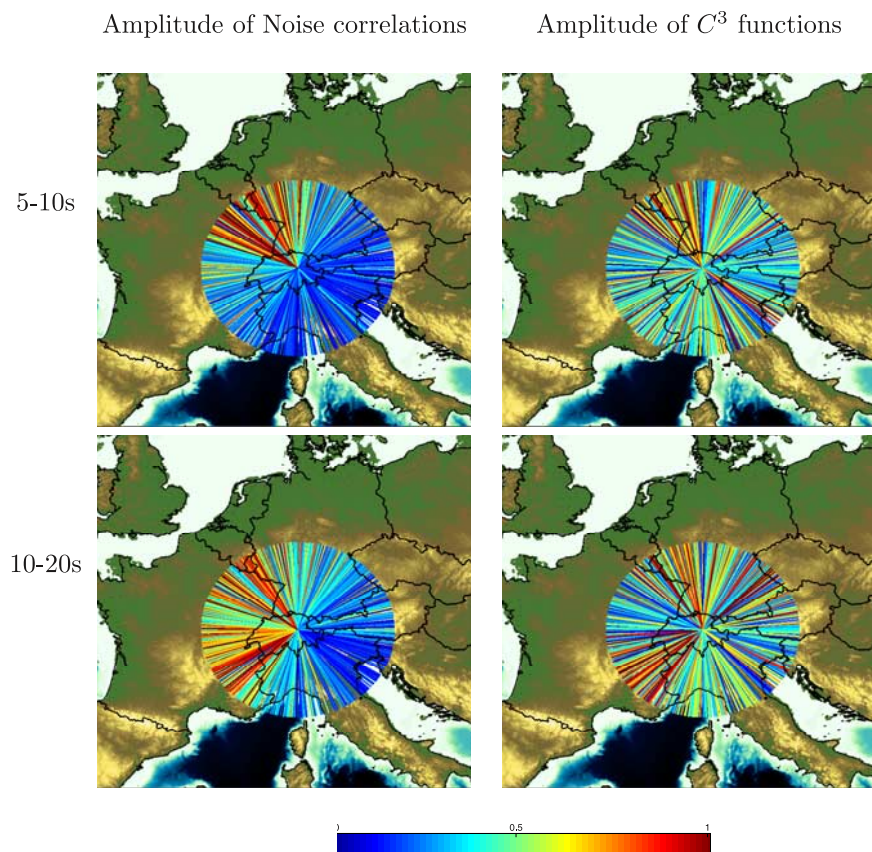


**Figure 4.** Amplitude versus azimuth of the Rayleigh wave part of the Green function obtained (left) from noise correlation and (right) from correlations of coda waves reconstructed by noise correlations for the two period bands (top) 5–10 s and (bottom) 10–20 s.

[31] Note that as discussed in section 2.2 we used only the  $C_{NN}$  and  $C_{PP}$  function. This means that the positive time of the  $C^3$  function corresponds to the causal Green's function of the medium between PLONS and ZUR, and the negative time to its anticausal counterpart. The gain of symmetry is therefore not an artefact of the signal processing but is due to the physics of waves propagation, namely the isotropization of the wavefield in the coda, and the process of averaging over the network. Moreover, the  $C_{II}^3$  functions are symmetric (Figure 3b, colored dashed lines). This means that the symmetry of the  $C^3$  function is not due to the fact that we selected coda waves on both positive and negative correlations times, since even when using only the coda on positive time (Figure 3b, blue dashed line) or on the negative time (Figure 3b, red dash-dotted line) the symmetry is preserved.

[32] As the Green's function reconstructed by coda waves correlations between PLONS-ZUR is symmetric it would be used in a tomographic study. This shows that correlations of correlations can be used to increase the number of paths where robust measurements of the arrival time of Rayleigh waves can be obtained, and thus contribute to increase the resolution of crustal images.

### 3.2. Interpretation

[33] When computing seismic noise correlations for the path PLONS-ZUR we used 1 year of continuous records. When computing  $C^3$  functions we used only 1200 s of coda

waves reconstructed by noise correlations, and the results was then averaged over 100 stations. This means that we used only 120,000 s of data, i.e., less than 2 days.

[34] Even if when computing  $C^3$  functions we use 100 times less data than when computing noise correlations it is still possible to have a better Green's function reconstruction for some paths like PLONS-ZUR because coda waves constitute a more isotropic field than the seismic ambient noise. Therefore the convergence of the correlations toward the Greens function is faster when using coda waves rather than seismic noise. This can be illustrated by plotting the amplitude of the correlations versus azimuth following the procedure of Stehly *et al.* [2006]. By measuring the amplitudes of Rayleigh waves reconstructed from noise correlations (respectively  $C^3$  functions) for all available station to station paths within positive and negative correlation times, we determine the average azimuthal distribution of seismic noise (respectively seismic coda) energy flow through the network. The results are presented in Figure 4. The amplitude of the noise correlations in the 5–10 s period band is clearly maximum for paths oriented in the northwest direction, i.e., facing the northern Atlantic Ocean: the noise recorded in Europe originates mainly from the northern Atlantic Ocean (Figure 4) and is therefore not isotropic. In the 10–20 s period band the noise as a wider azimuthal distribution but is still largely dominated by noise coming from the Atlantic Ocean. On the other hand, the amplitude of the Rayleigh waves obtained from  $C^3$

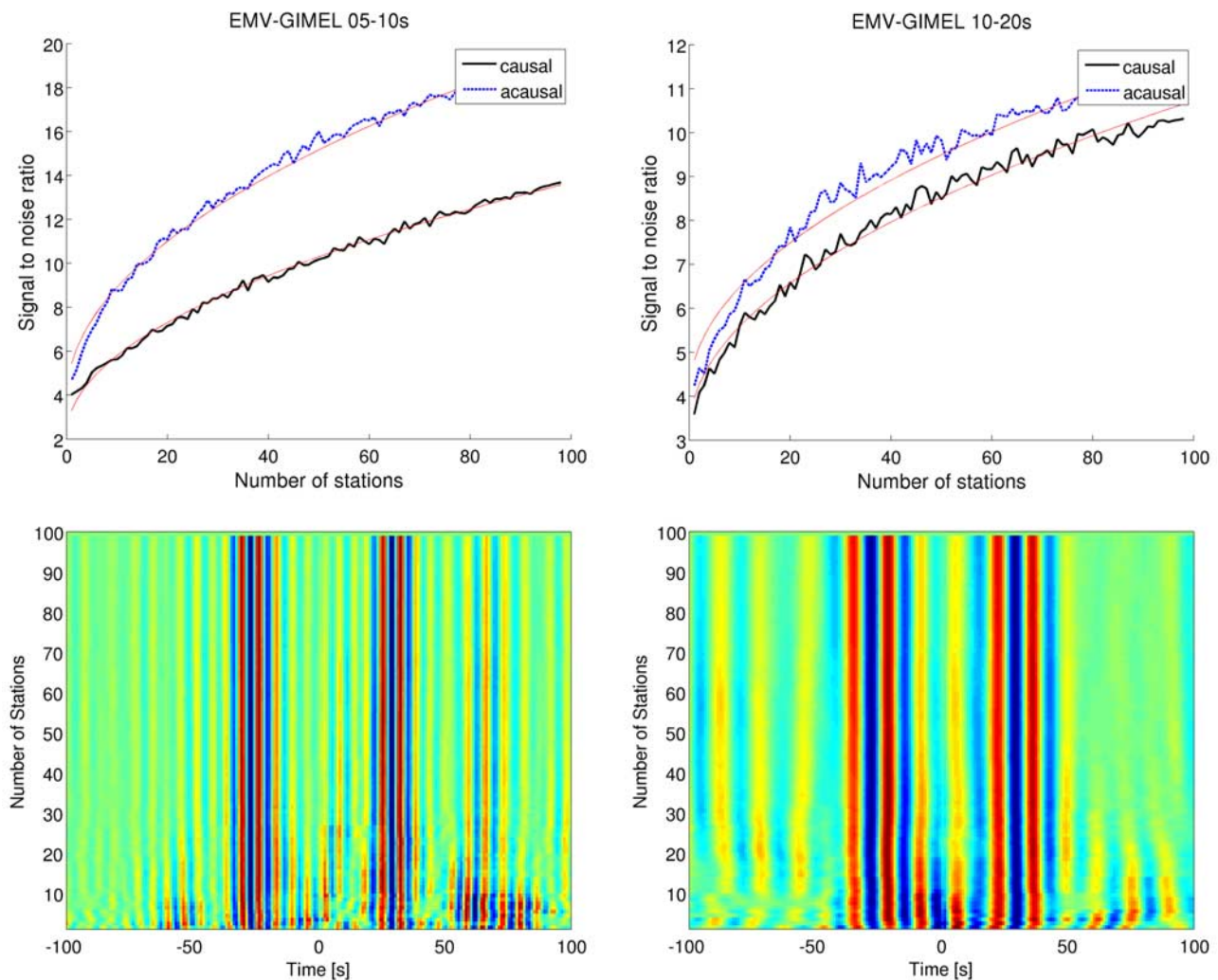


**Figure A1.** (a and b) Signal-to-noise ratio of the  $C^3$  function versus the number of stations used for the path EMV-GIMEL in the 5–10 s and 10–20 s period bands, respectively. Results are shown with a black solid lines for positive times of the  $C^3$  function and with a blue dashed lines for negative times. The signal-to-noise ratio evolves as a function proportional the square root of the number of stations used shown in red. (c and d)  $C^3$  functions versus the number of stations used in the 5–10 s and 10–20 s period band.

functions does not depend on the azimuth (Figure 4). By using coda waves from noise correlation we get ride off the nonisotropic distribution of noise sources. Therefore the quality of the Green's function reconstruction doesn't depend anymore on the azimuth as with seismic noise. This is why it is possible to reconstruct the Green's function of the medium with  $C^3$  functions for paths where noise correlations does not give any results.

#### 4. Conclusion

[35] We showed experimentally that a metacorrelation, that is a correlation of (the coda of) ambient noise correlations can be used to construct direct arrivals between two stations even when the stations are badly oriented with respect to ambient noise flux. The success of the technique is an indication that correlations of ambient noise are meaningful at large lag time; their codas contain multiply scattered waves. These waves have the expected properties

for retrieving the Green's functions [Lobkis and Weaver, 2001; Campillo and Paul, 2003]. While these contributions are small and difficult to identify in individual noise correlations, their correlations are enhanced by averaging over a network in the form of clear direct arrivals. Further developments would ideally use iteratively this approach to improve the signal-to-noise ratio of the Green's function reconstruction.

#### Appendix A

[36] For practical applications, it is useful to know what is the convergence rate of the  $C^3$  functions toward the Green's function: How many stations do we need to reconstruct accurately the Green's function? What is the optimal length of coda that should be used?

[37] The answers depend on several parameters such as the geometry of the network, the distribution of the noise sources, the scattering of the medium. Rigorously studying

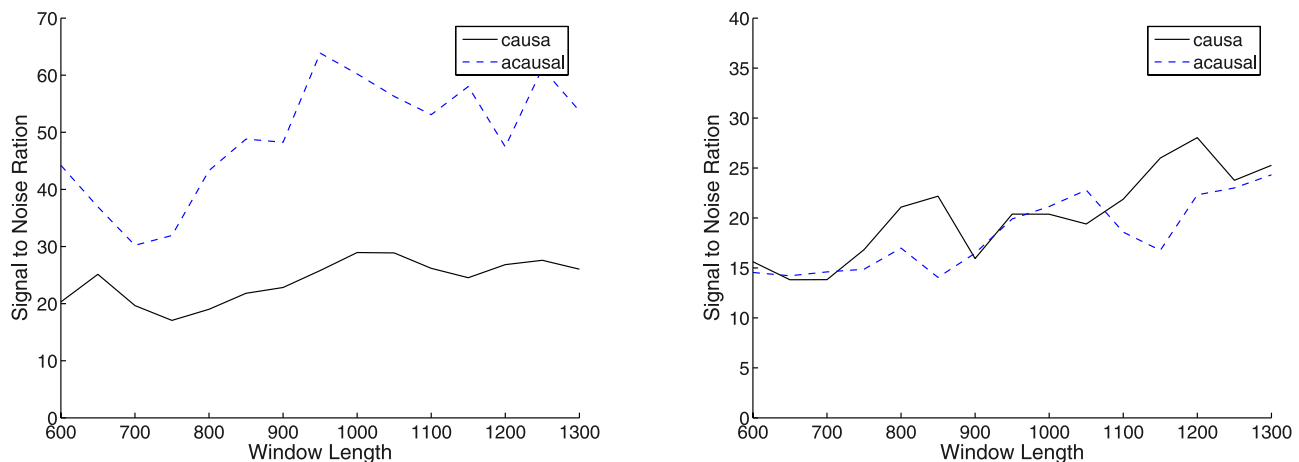


**Figure A2.** Signal-to-noise ratio of the  $C^3$  function between PLONS and ZUR versus the length of the coda window used for the (left) 5–10 s period band and (right) 10–20 s period band.

this question is out of scope of this article, but we would like to show how the signal-to-noise ratio of the  $C^3$  function evolves with the number of stations and the length of the coda window used. This gives a first idea about what kind of networks are suitable to compute  $C^3$  functions.

[38] Figures A1a and A1b show how the signal-to-noise ratio (SNR) of the  $C^3$  function computed between EMV and GIMEL increases with the number of stations used. We define signal-to-noise ratio as the ratio of the amplitude of the Rayleigh wave and the variance of the noise following Rayleigh waves. More precisely, the variance of the noise is evaluated in a time window that starts at arrival time of the Rayleigh waves plus 100 s and finish at 1200 s. The signal-to-noise ratio is measured separately on the positive and negative correlation time. It is known that the signal-to-noise ratio of noise correlations evolves as the square root of the amount of data used when noise sources are evenly distributed within the medium [Larose *et al.*, 2004; Snieder, 2004; Sabra *et al.*, 2005a; Weaver and Lobkis, 2005]. Similarly, we found that the signal-to-noise ratio of the  $C^3$  function is proportional to the square root of the number of station used (i.e., to the length of signal correlated). The coefficient of proportionality is not the same in the 5–10 s and 10–20 s period band for positive and negative time.

[39] Figures A1c and A1d show how the waveforms of the  $C^3$  function evolves with the number of stations used in the 5–10 s and 10–20 s period band. When using only 10 stations, Rayleigh waves are already clearly visible but with a signal-to-noise ratio too slow to measure accurately their travel times. On the other hand when using more than 40 stations, the measured arrival time of Rayleigh waves doesn't change anymore when adding more stations and the signal-to-noise ratio of the  $C^3$  function is greater than 10, in the two period band on positive and negative time.

[40] These results indicates that for the path EMV-GIMEL whose range is 71 km about 40 stations are required to reconstruct the Green's function accurately in the 5–10 and 10–20 s period band. When considering larger distances, we expect that more stations should be used.

[41] Figure A2 shows how the signal-to-noise ratio of the  $C^3$  function between PLONS and ZUR depends on the length of the coda windows  $\Delta t$  used, when considering all

the stations of the network. In this case the signal-to-noise ratio is defined as the ratio of the variance of the Rayleigh waves and the variance of the noise following coda waves on the  $C^3$  function. The variance of the noise is evaluated in a window starting at 80% of the coda windows length –50 s and last at 100 s. This definition makes it possible to compare the signal-to-noise ratio of the  $C^3$  function computed with different coda windows.

[42] In the 5–10 s period band the signal-to-noise ratio of the  $C^3$  function is maximized when using 1000 s of coda. In the 10–20 s period band keeps on increasing when increasing the length of the coda windows.

[43] **Acknowledgments.** All the seismic data used in this study have been obtained from the IRIS DMC (<http://www.iris.edu/>), the ORFEUS database (<http://www.orfeus-eu.org/>), the ETH Zürich, the Commissariat à l'Énergie Atomique (CEA, France), and the LGIT. This research has been supported by the Commissariat à l'Énergie Atomique (CEA, France), by the European Community (project NERIES), and by ANR (France) under contracts 05-CATT-010-01 (PRECORISIS).

## References

- Brenguier, F., N. M. Shapiro, M. Campillo, A. Nercessian, and V. Ferrazzini (2007), 3-D surface wave tomography of the Piton de la Fournaise volcanic using seismic noise correlations, *Geophys. Res. Lett.*, *34*, L02305, doi:10.1029/2006GL028586.
- Brenguier, F., N. Shapiro, M. Campillo, V. Ferrazzini, Z. Duputel, O. Coutant, and A. Nercessian (2008), Towards forecasting volcanic eruptions using seismic noise, *Nat. Geosci.*, *1*, 126–130, doi:10.1038/ngeo104.
- Campillo, M. (2006), Phase and correlation in 'random' seismic fields and the reconstruction of the Green's function, *Pure Appl. Geophys.*, *163*, 475–502, doi:10.1007/s00024-005-0032-8.
- Campillo, M., and A. Paul (2003), Long-range correlations in the diffuse seismic coda, *Science*, *299*, 547–549, doi:10.1126/science.1078551.
- Duvall, T. L., S. M. Jefferies, J. W. Harvey, and M. A. Pomerantz (1993), Time distance helioseismology, *Nature*, *362*, 430–432.
- Gizon, L., and A. C. Birch (2004), Time-distance helioseismology: noise estimation, *Astrophys. J.*, *614*, 472–489.
- Gizon, L., and A. C. Birch (2005), Local helioseismology, *Living Rev. Sol. Phys.*, *2*, <http://solarphysics.livingreviews.org/Articles/lrsp-2005-6/>.
- Gouédard, P., et al. (2008), Cross-correlation of random fields: Mathematical approach and applications, *Geophys. Prospect.*, *56*, 375–393, doi:10.1111/j.1365-2478.2007.00684.x.
- Hennino, R., N. Tégoures, N. Shapiro, L. Margerin, M. Campillo, B. van Tiggelen, and R. Weaver (2001), Observation of equipartition of seismic waves, *Phys. Rev. Lett.*, *85*(15), 3447–3450.
- Kedar, S., M. Longuet-Higgins, F. Webb, N. Graham, R. Clayton, and C. Jones (2008), The origin of deep ocean microseisms in the North

- Atlantic Ocean, *Proc. R. Soc., Ser. A*, 464(2091), 777–793, doi:10.1098/rspa.2007.0277.
- Larose, E., A. Derode, M. Campillo, and M. Fink (2004), Imaging from one-bit correlation of wide-band diffuse wavefield, *J. Appl. Phys.*, 95, 8393–8399.
- Larose, E., L. Margerin, A. Derode, B. V. Tiggelen, M. Campillo, N. M. Shapiro, A. Paul, L. Stehly, and M. Tanter (2006), Correlation of random wavefields: an interdisciplinary review, *Geophysics*, 71(4), SI11–SI21.
- Lin, F., M. H. Ritzwoller, J. Townend, M. Savage, and S. Bannister (2007), Ambient noise Rayleigh wave tomography of New Zealand, *Geophys. J. Int.*, (18), 649–666, doi:10.1111/j.1365-246X.2007.03414.x.
- Lobkis, O. I., and R. L. Weaver (2001), On the emergence of the Green's function in the correlations of a diffuse field, *J. Acoust. Soc. Am.*, 110, 3011–3017.
- Louquet-Higgins, M. (1950), A theory of the origin of microseisms, *Philos. Trans. R. Soc. London*, 243, 137–171.
- Paul, A., M. Campillo, L. Margerin, E. Larose, and A. Derode (2005), Empirical synthesis of time-asymmetrical Green's functions from the correlation of coda waves, *J. Geophys. Res.*, 110, B08302, doi:10.1029/2004JB003521.
- Roux, P., K. G. Sabra, W. A. Kuperman, and A. Roux (2005), Ambient noise cross correlation in free space: Theoretical approach, *J. Acoust. Soc. Am.*, 117(1), 79–84, doi:10.1121/1.1830673.
- Sabra, K., P. Roux, and W. Kuperman (2005a), Emergence rate of the time-domain Green's function from the ambient noise cross-correlation, *J. Acoust. Soc. Am.*, 118(6), 3524–3531, doi:10.1121/1.2109059.
- Sabra, K. G., P. Gerstoft, P. Roux, W. A. Kuperman, and M. C. Fehler (2005b), Surface wave tomography from microseisms in southern California, *Geophys. Res. Lett.*, 32, L14311, doi:10.1029/2005GL023155.
- Sánchez-Sesma, F. J., J. A. Pérez-Ruiz, M. Campillo, and F. Luzón (2006), Elastodynamic 2D Green's function retrieval from cross-correlation: Canonical inclusion problem, *Geophys. Res. Lett.*, 33, L13305, doi:10.1029/2006GL026454.
- Sens-Schönfelder, C., and U. Wegler (2006), Passive image interferometry and seasonal variations of seismic velocities at Merapi Volcano, Indonesia, *Geophys. Res. Lett.*, 33, L21302, doi:10.1029/2006GL027797.
- Shapiro, N. M., M. Campillo, L. Margerin, S. K. Singh, V. Kostoglodov, and J. Pacheco (2000), The energy partitioning and the diffusive character of the seismic coda, *Bull. Seismol. Soc. Am.*, 90, 655–665.
- Shapiro, N. M., M. Campillo, L. Stehly, and M. H. Ritzwoller (2005), High-resolution surface wave tomography from ambient seismic noise, *Science*, 307, 1615–1618.
- Snieder, R. (2004), Extracting the Green's function from the correlation of coda waves: A derivation based on stationary phase, *Phys. Rev. E*, 69, 046610, doi:10.1103/PhysRevE.69.046610.
- Snieder, R. (2007), Extracting the green's function of attenuating heterogeneous acoustic media from uncorrelated waves, *J. Acoust. Soc. Am.*, 121(5), 2637–2642.
- Stehly, L., M. Campillo, and N. M. Shapiro (2006), A study of the seismic noise from its long-range correlation properties, *J. Geophys. Res.*, 111, B10306, doi:10.1029/2005JB004237.
- Wapenaar, K. (2004), Retrieving the elastodynamic Green's Function of an arbitrary inhomogeneous medium by cross-correlation, *Phys. Rev. Lett.*, 93, 254301, doi:10.1103/PhysRevLett.93.254301.
- Weaver, R. L. (2008), Ward identities and the retrieval of the Greens functions in the correlations of a diffuse field, *Wave Motion*, 45, 596–604.
- Weaver, R. L., and O. I. Lobkis (2001), Ultrasonics without a source: thermal fluctuation correlations at MHz frequencies, *Phys. Rev. Lett.*, 87(13), 134301, doi:10.1103/PhysRevLett.87.134301.
- Weaver, R. L., and O. I. Lobkis (2004), Diffuse waves in open systems and the emergence of the Green's function, *J. Acoust. Soc. Am.*, 116(5), 2731–2734, doi:10.1121/1.1810232.
- Weaver, R. L., and O. I. Lobkis (2005), Fluctuations in diffuse field-field correlations and the emergence of the Green's function in open systems, *J. Acoust. Soc. Am.*, 117, 3432–3439, doi:10.1121/1.1898683.
- Wegler, U., and C. Sens-Schönfelder (2007), Fault zone monitoring with passive image interferometry, *Geophys. J. Int.*, 168(3), 1029–1033, doi:10.1111/j.1365-246X.2006.03284.x.
- Yang, Y., M. H. Ritzwoller, A. L. Levshin, and N. M. Shapiro (2007), Ambient noise Rayleigh wave tomography across Europe, *Geophys. J. Int.*, 168, 259–274, doi:10.1111/j.1365-246X.2006.03203.x.
- Yao, H., R. D. van der Hilst, and M. V. de Hoop (2006), Surface-wave array tomography in SE Tibet from ambient seismic noise and two-station analysis – I. Phase velocity maps, *Geophys. J. Int.*, 166, 732–744, doi:10.1111/j.1365-246X.2006.03028.x.

---

M. Campillo and B. Froment, LGIT, Université Joseph Fourier, BP 53, CNRS, F-38041 Grenoble, France.

L. Stehly, Berkeley Seismological Laboratory, University of California, 209 McCone Hall, Berkeley, CA 94720, USA. (lstehtly@seismo.berkeley.edu)

R. L. Weaver, Department of Physics, University of Illinois at Urbana-Champaign, 1110 W. Green Street, Urbana, IL 61801, USA.